Reprinted from SPIE Vol. 767—Medical Imaging

Analysis of DQE and NEQ measurement errors for medical imaging systems

Peter D. Burns

Research Laboratories - Commercial and Information Systems Group
Eastman Kodak Company, Rochester, New York 14650

Abstract

Recent work aimed at quantifying the statistical efficiency of diagnostic imaging systems has resulted in the frequent use of the detective quantum efficiency (DQE) and noise equivalent quantum exposure (NEQ). Estimation of these metrics requires the separate measurement of several imaging parameters. An analysis is given which results in expressions for DQE and NEQ estimate errors in terms of component measurement error statistics.

Introduction

The efficiency with which image information is captured by an image detector is often expressed in terms of its detective quantum efficiency (DQE). The corresponding description of signal-to-noise ratio, for quantum limited exposure applications, is the noise equivalent quantum exposure (NEQ). These metrics were originally applied to photographic film[1-3] and video cameras.[4] More recently they have been used to quantify the performance of various medical imaging systems, including x-ray screen-film[5,6], ultrasound, nuclear medicine[7] and xeroradiography.[8,9] The utility of this approach has been demonstrated both in the development of physical models,[10,11] and the comparison of various diagnostic imaging systems and modalities.[7,12,13]

The DQE is defined as the ratio of the output (D) and input exposure (Q) variances when they are expressed in equivalent units via the system (mean signal) transfer characteristic,[14]

$$DQE = \frac{\sigma_Q^2}{\sigma_D^2} G^2,$$

where G=dD/dQ. The NEQ is

$$NEQ = Q\ DQE,$$

where Q is the mean exposure. Since for the quantum input, $\sigma_Q{}^2 = Q$,

$$DQE(Q) = \frac{Q}{\sigma_D^2(Q)} G^2(Q).$$

In general, both DQE and NEQ are also functions of spatial frequency (ω). They can, therefore, be expressed in terms of the system MTF (T) and Wiener, or noise power, spectrum (S):[3]

$$DQE(Q,\omega) = \frac{Q\,[T(Q,\omega)\,G(Q)]^2}{S(Q,\omega)} \qquad (1)$$

$$NEQ(Q,\omega) = \frac{[Q\,T(Q,\omega)\,G(Q)]^2}{S(Q,\omega)}. \tag{2}$$

Since the sensitometric properties of photographic imaging systems are expressed in terms of a density-log exposure function, equations (1) and (2) are usually written

$$DQE(Q,\omega) = \frac{[log_{10}e\,T(Q,\omega)\,\gamma(Q)]^2}{Q\,S(Q,\omega)} \tag{3}$$

$$NEQ(Q,\omega) = \frac{[log_{10}e\,T(Q,\omega)\,\gamma(Q)]^2}{S(Q,\omega)}, \tag{4}$$

where $\gamma(Q) = dD/dlog_{10}Q$.

Knowledge of measurement errors aids in the interpretation of results, particularly when making comparisons with model predictions.[15] Estimation of DQE and NEQ require the separate measurement of several parameters, including those describing signal transfer (γ, T) and image noise (S) characteristics. The results of these measurements are then combined as in equations (3) and (4) to give the DQE and NEQ estimates.* Errors associated with each component measurement will, therefore, combine to determine the accuracy and precision of the final estimates. A common statistical measure of the accuracy of an estimate is its bias, defined as the expected value minus the true value

$$b_{DQE}(Q,\omega) = E[\widehat{DQE}(Q,\omega)] - \mu_{DQE}(Q,\omega), \tag{5}$$

where $\widehat{DQE}$ is the estimated DQE value, μ_{DQE} is the true value, and E is the statistical expectation. The variance (or its square root) is a measure of the precision of the estimate

$$\sigma^2_{DQE}(Q,\omega) = E[\widehat{DQE}^2(Q,\omega)] - \mu^2_{DQE}(Q,\omega). \tag{6}$$

The bias and variance combine to determine the root mean square (RMS) error

$$RMS_{DQE}(Q,\omega) = [\sigma^2_{DQE}(Q,\omega) + b^2_{DQE}(Q,\omega)]^{\frac{1}{2}}. \tag{7}$$

In this report, errors associated with DQE and NEQ estimates will be expressed in terms of the statistics of the errors in the component measurements of γ, MTF, etc. The error associated with any measurement can result from several sources such as instrument calibration and noise, image nonuniformity, and image noise. Results of recent efforts to reduce effective microdensitometer noise are reported in these proceedings.[16,17] Before the DQE and NEQ measurement errors are addressed, we briefly describe the required component measurements and their associated sources of error. No explicit discussion of estimate smoothing is included. However, smoothing techniques can be evaluated in terms of their effect on the variance, bias, and RMS error of the resulting DQE and NEQ estimates. We restrict our attention to the first and second statistical moments of the various errors.

Measurements

Sensitometric characteristics are evaluated by modulating either exposure time or intensity.[18,19] Quantitative comparison of several techniques applied to x-ray screen-film [20–22] indicate generally good agreement of the density-log exposure characteristics despite such error sources as reciprocity law failure, spectral matching of artificial and clinical sources, and scattering. The variation between the results of different methods has been reported to be about 2-3%. It should be noted that these errors refer to measurements of relative exposure. Absolute exposure measurement requires the calibration of the exposure source. A

* MTF, Wiener spectra, etc. are estimated from physical measurements. For the purposes of this report, however, we will refer to DQE and NEQ *estimates* based on *measurements* of Q, γ, T and S.

calibrated ionization chamber is used to measure the x-ray exposures. The resultant milliroentgen data are then expressed in terms of an estimated quantum fluence via x-ray spectrum data.[23] Errors associated with this procedure contribute to errors in the measurement of absolute sensitometry.

MTF evaluation usually requires scanning the image of either an edge,[13] slit,[24] or square-wave [25,26] target. The scanned data is expressed in terms of an inferred input exposure via the characteristic function. Variation in this function naturally leads to errors in the line spread function (LSF) and MTF.[27] For density values where the derivative of the characteristic curve is low (i.e. at the toe), estimation of input exposure is less accurate. To reduce this error and avoid truncation of the LSF, multiple measurements can be made with several peak exposure values.[28–30] Truncation of the line spread function must be avoided since this leads to systematic MTF (bias) errors. Alternatively, pre-exposure can be used.[31] In addition, systematic errors can also be caused by misallignment of the measurement aperture [32] and aliasing.[24,33]

The reduction of stochastic errors in MTF measurements is often accomplished by averaging of several measurement scans. In addition, fitting the MTF to smooth curves may be useful since the measured MTF is then described by a small number of parameters. Empirical curve fitting can introduce bias errors but useful results for screen-film MTFs have been reported.[34,35]

The two-dimensional Wiener spectrum is usually represented as an isotropic function of a single spatial frequency. This measurement requires the repeated sampling of a uniformly exposed image with a measuring slit of appropriate length.[36] Of the various methods available for estimating the one-dimensional Wiener spectrum,[37] those based on the periodogram are widely applied to diagnostic image noise.[24,38] Other Wiener spectrum estimation methods have recently been described including a two-dimensional periodogram,[39] maximum entropy estimation of an autoregressive model,[40] and optical autocorrelator.[41] Image nonuniformity or other artifacts introduce significant errors into the Wiener spectrum measurement, particularly at low spatial frequencies. To reduce the positive bias errors associated with image nonuniformity, the original data is sometimes detrended [42] or otherwise filtered.[12,37] Statistical tests of the mean and variance can also be used to detect certain types of image nonuniformity.[43]

The final step in estimating the Wiener spectrum is to express the function in terms of absolute diffuse density. This requires characterizing the microdensitometer instrument (specular) density-diffuse density relationship. The Wiener spectrum estimate is corrected via the square of the slope of this calibration curve.[44] Errors associated with measurement of the slope of the calibration curve as low as 1.5% rms and total Wiener spectrum errors of 10% have been reported.[45]

DQE and NEQ estimation errors

DQE and NEQ are not measured directly but inferred from the results of several physical image measurements. DQE and NEQ values are estimated via expressions (algorithms) such as equations (1) and (2) or (3) and (4). We will consider them to be statistical parameters to be estimated, much like the mean or autocovariance function. The DQE value can be estimated at exposure Q and spatial frequency ω by

$$\widehat{DQE}(Q,\omega) = \frac{[log_{10}e\,\hat{\gamma}(Q)\,\hat{T}(Q,\omega)]^2}{\hat{Q}\,\hat{S}(Q,\omega)} \tag{8}$$

where circumflex ($\hat{}$) indicates a measured value or an estimate based on measurements. Each measured value has an associated error which we model as the sum of a constant bias and a zero-mean random variable. For $\hat{\gamma}$ this is written

$$\hat{\gamma}_i(Q) = \mu_\gamma(Q) + b_\gamma(Q) + \Delta\gamma_i(Q), \tag{9}$$

where i indicates the ith measurement realization, μ_γ is the true value, and b_γ is the bias given by

$$b_\gamma(Q) = E[\hat{\gamma}(Q)] - \mu_\gamma(Q). \tag{10}$$

The zero-mean error is $\Delta\gamma$ with variance $\sigma^2_\gamma(Q)$. The other measurements are expressed in the same way, suppressing the arguments Q and ω :

$$\hat{T}_i = \mu_T + b_T + \Delta T_i$$

$$\hat{Q}_i = \mu_Q + b_Q + \Delta Q_i \tag{11}$$
$$\hat{S}_i = \mu_S + b_S + \Delta S_i.$$

We will assume that the stochastic measurement error sources are independent. Therefore, the expectation for the product of any combination of them is zero:

$$E[\Delta\gamma\,\Delta T] = E[\Delta\gamma\,\Delta S] = E[\Delta\gamma\,\Delta T\,\Delta S]\ldots = 0.$$

We start with the simplest case of unbiased measurements. For this case, b_Q, b_γ, etc. are zero. We can expand the function $\widehat{DQE}$ in a Taylor series about the true values and take expectations.[46] Using the results of Appendix I, the expected value is

$$E[\widehat{DQE}] = \mu_{DQE} + \mu_{DQE}\left\{\frac{\sigma_\gamma^2}{\mu_\gamma^2} + \frac{\sigma_T^2}{\mu_T^2} + \frac{\sigma_Q^2}{\mu_Q^2} + \frac{\sigma_S^2}{\mu_S^2}\right\}, \tag{12}$$

where

$$\mu_{DQE} = \frac{[log_{10}e\;\mu_\gamma\;\mu_T]^2}{\mu_Q\;\mu_S}.$$

The bias of the DQE estimate is the second term of equation (12),

$$b1_{DQE} = \mu_{DQE}\left\{\frac{\sigma_\gamma^2}{\mu_\gamma^2} + \frac{\sigma_T^2}{\mu_T^2} + \frac{\sigma_Q^2}{\mu_Q^2} + \frac{\sigma_S^2}{\mu_S^2}\right\}. \tag{13}$$

The same approach leads to the expression for the variance (Appendix I):

$$\sigma_{DQE}^2 = \mu_{DQE}^2\left\{\frac{4\sigma_\gamma^2}{\mu_\gamma^2} + \frac{4\sigma_T^2}{\mu_T^2} + \frac{\sigma_Q^2}{\mu_Q^2} + \frac{\sigma_S^2}{\mu_S^2}\right\}. \tag{14}$$

The corresponding expressions for the bias and variance of the NEQ estimate are

$$b1_{NEQ} = \mu_{NEQ}\left\{\frac{\sigma_\gamma^2}{\mu_\gamma^2} + \frac{\sigma_T^2}{\mu_T^2} + \frac{\sigma_S^2}{\mu_S^2}\right\} \tag{15}$$

$$\sigma_{NEQ}^2 = \mu_{NEQ}^2\left\{\frac{4\sigma_\gamma^2}{\mu_\gamma^2} + \frac{4\sigma_T^2}{\mu_T^2} + \frac{\sigma_S^2}{\mu_S^2}\right\}. \tag{16}$$

For the special case where all measurement errors have zero mean with standard deviation an equal constant fraction, K, of the true value, then from equations (14) and (16)

$$\frac{\sigma_{DQE}}{\mu_{DQE}} = \sqrt{10}\;K\;, \quad \frac{\sigma_{NEQ}}{\mu_{NEQ}} = 3\;K.$$

If the measurements used to estimate the DQE contain bias errors, as in equations (9) and (11), there will be an additional bias in $\widehat{DQE}$. From Appendix II this bias, $b2_{DQE}$, is given approximately by

$$b2_{DQE} \approx \mu_{DQE}\left\{\frac{2b_T}{\mu_T} + \frac{2b_\gamma}{\mu_\gamma} - \frac{b_Q}{\mu_Q} - \frac{b_S}{\mu_S}\right\}. \tag{17}$$

The corresponding expression for $b2_{NEQ}$ is

$$b2_{NEQ} \approx \mu_{NEQ}\left\{\frac{2b_\gamma}{\mu_T} + \frac{2b_T}{\mu_T} - \frac{b_S}{\mu_S}\right\}. \tag{18}$$

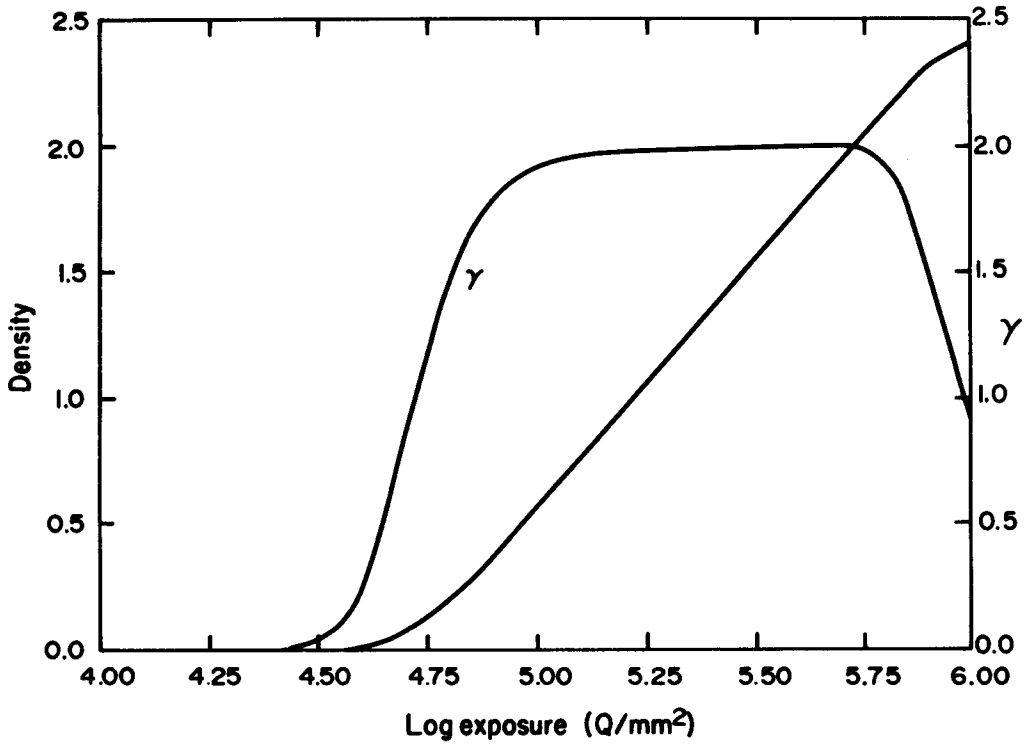

Figure 1: Sensitometry of computed example.

For the general case of biased stochastic errors, comparison of equations (13) and (17) to (15) and (18) indicate that component measurement bias is a much more serious contributor to DQE (NEQ) bias than measurement variation. The variance of the DQE and NEQ estimates based on biased measurements remains unchanged from the unbiased result of equations (14) and (16). The above results show that the moments of the measurements combine simply to determine b_{DQE} and σ_{DQE} when expressed as a fraction of the true value, or coefficient of variation. It should be emphasized that this relative error will usually vary with Q and ω.

Computed example

The above results will now be used in a sample calculation of the errors associated with the DQE estimate. The imaging system to be evaluated has a characteristic curve as given in Figure 1. The errors associated with measurement of absolute exposure and γ are unbiased and proportional to the true values, $\sigma_Q = 0.05\ \mu_Q$ and $\sigma_\gamma = 0.03\ \mu_\gamma$. The system MTF is given in figure 2. The measured MTF is subject to unbiased stochastic errors ($\sigma_T = 0.02$), independent of spatial frequency. The Wiener spectrum is shown in figure 3 plotted versus log exposure and spatial frequency. We will assume a proportional stochastic error, $\sigma_S = 0.08\ \mu_s$, with a bias due to the measuring instrument and image nonuniformity as shown in figure 4.

The resulting true DQE surface is shown in Figure 5. The standard deviation and bias of the DQE estimate, σ_{DQE} and b_{DQE} are plotted in Figures 6 and 7. The bias is negative due to the positive bias of the measured Wiener spectrum [equation (17)]. The shape of the total RMS error, given in Figure 8, resembles that of the true DQE, since most of the stochastic error sources are proportional to their respective true values.

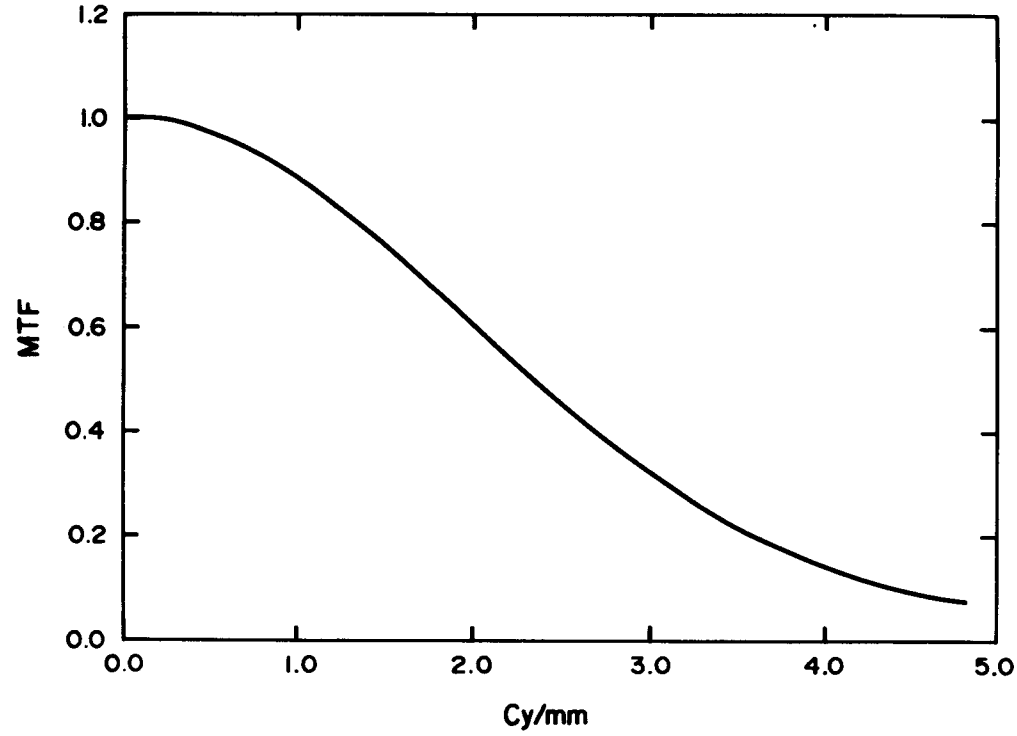

Figure 2: Example MTF.

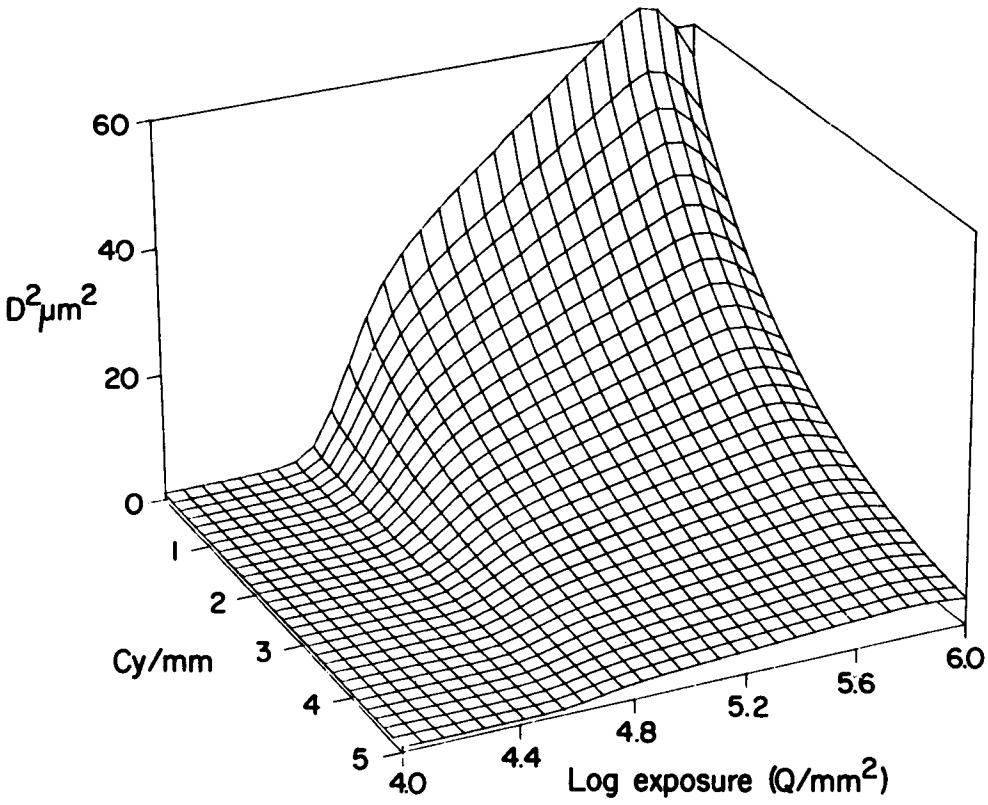

Figure 3: Wiener spectrum of computed example.

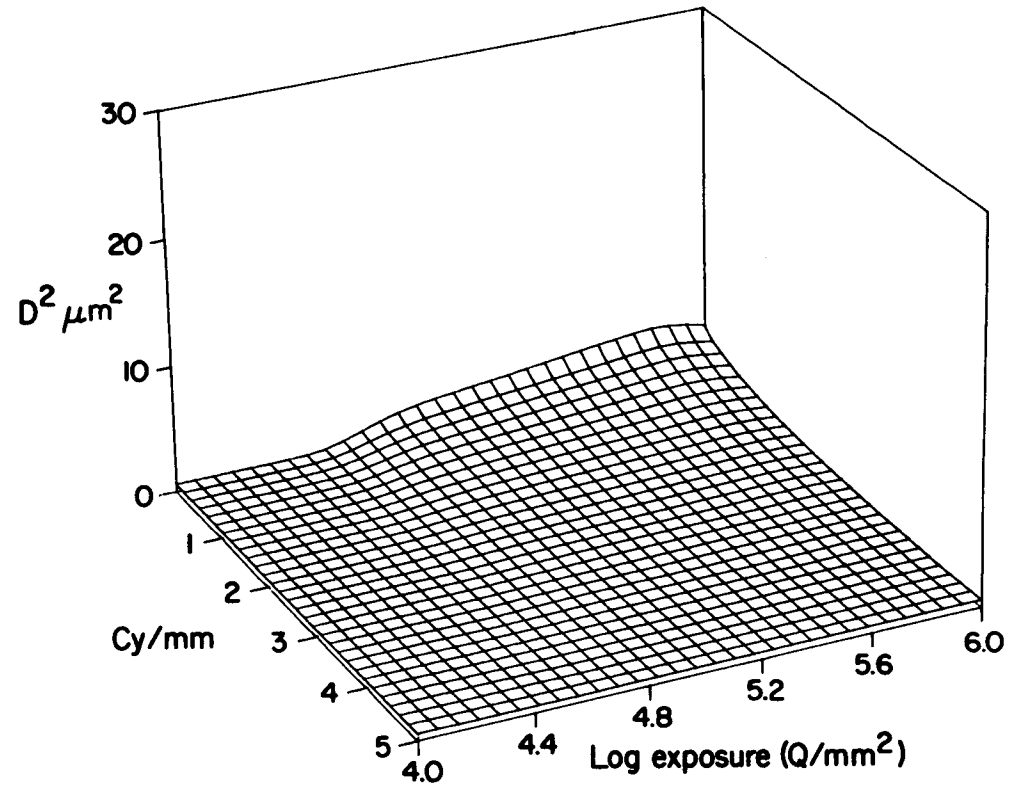

Figure 4: Bias of the Wiener spectrum measurement.

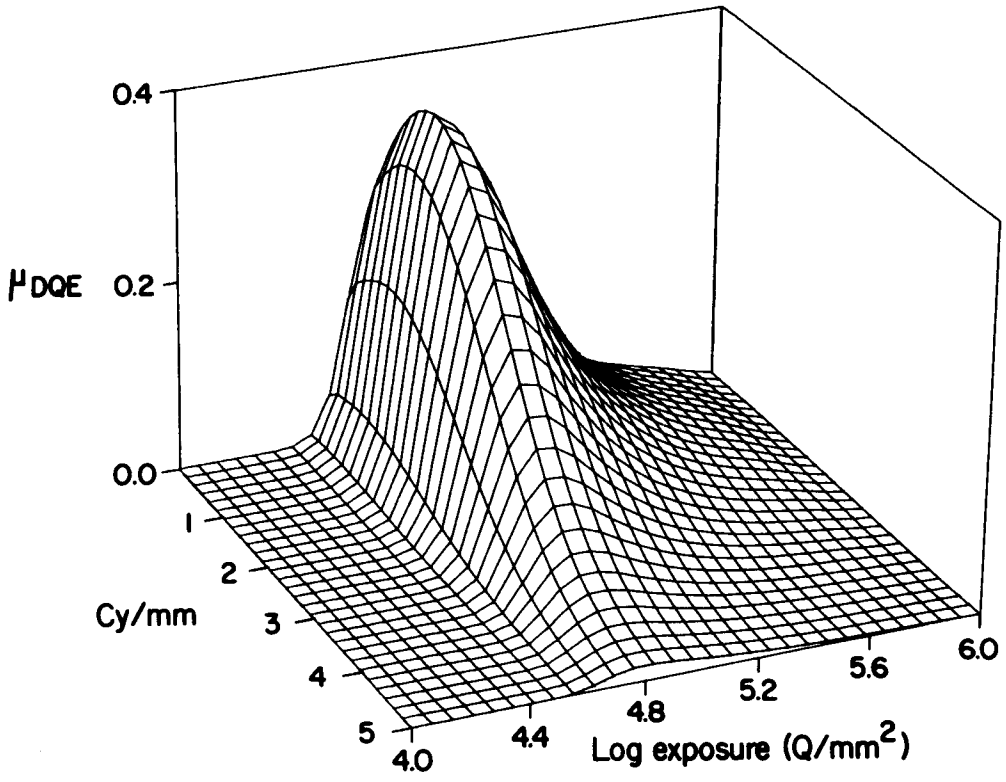

Figure 5: DQE surface of the example.

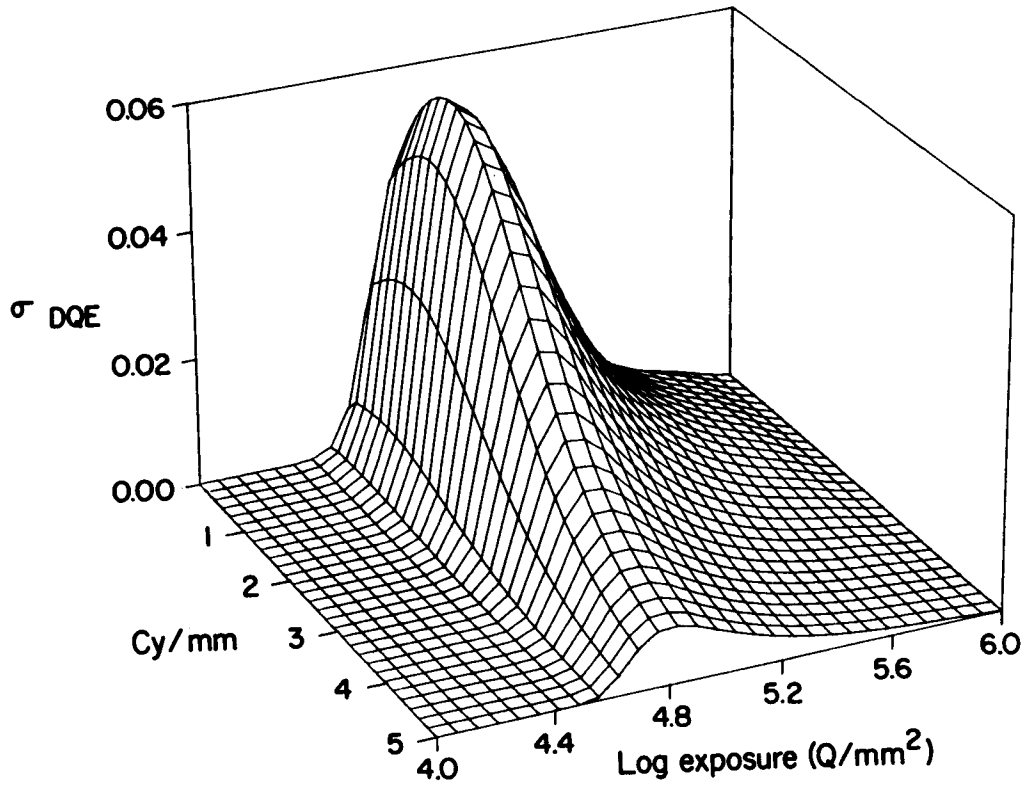

Figure 6: Standard deviation of DQE estimate.

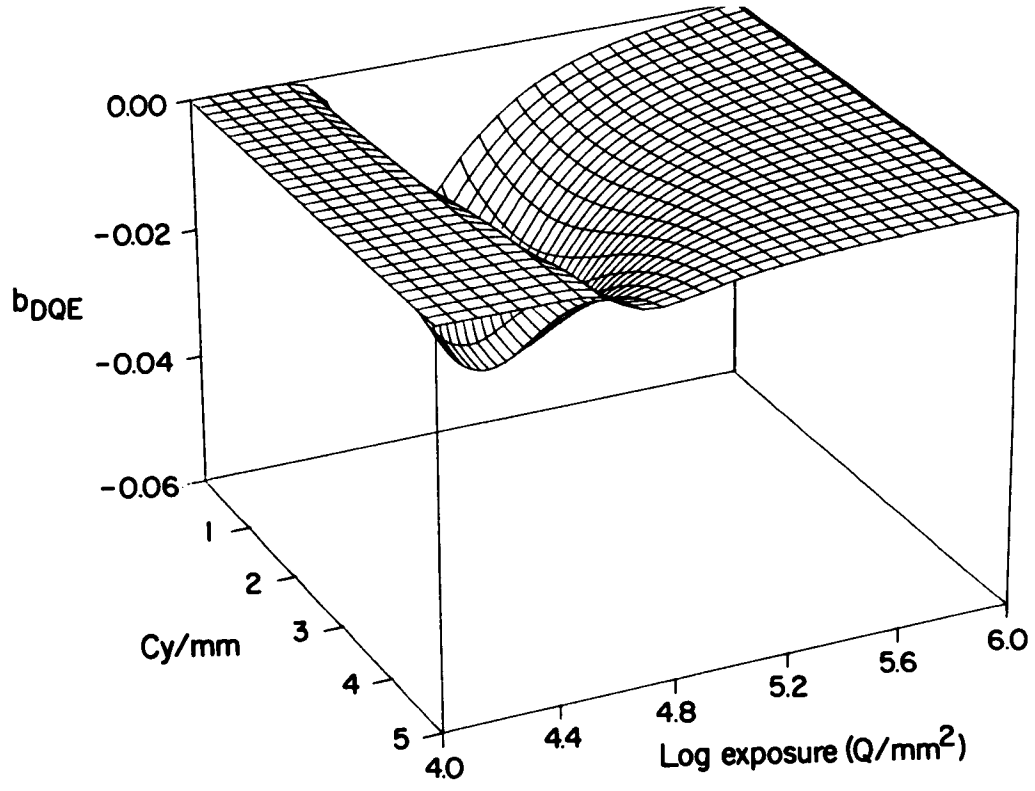

Figure 7: Bias of DQE estimate.

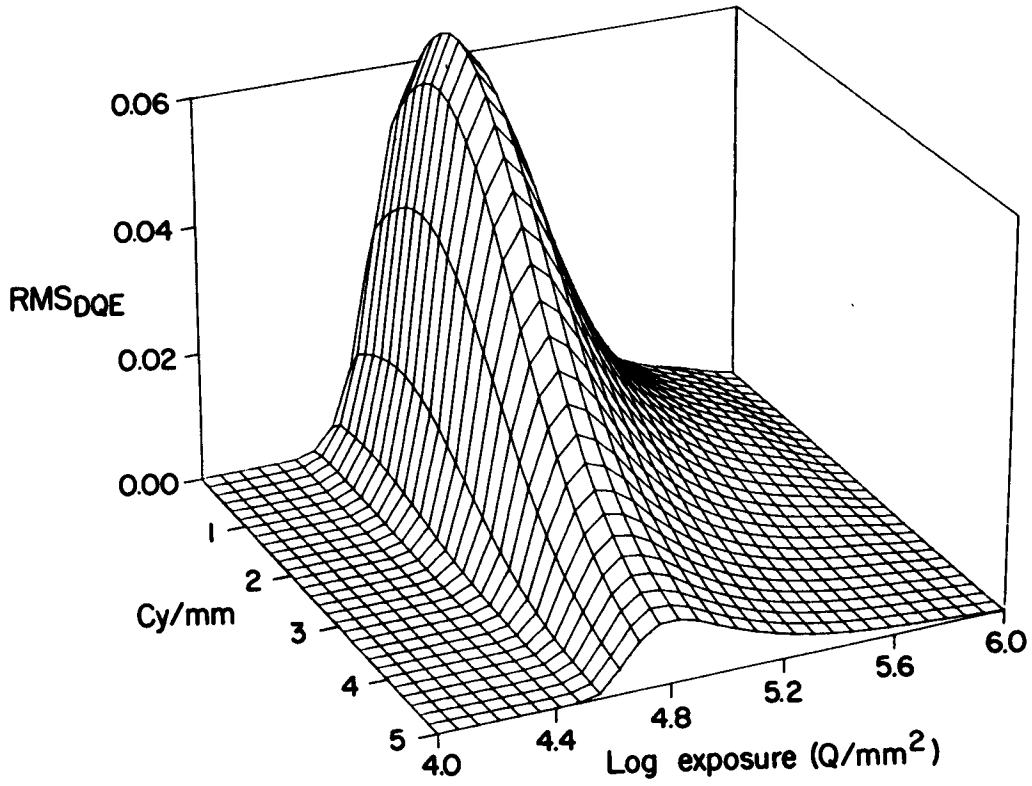

Figure 8: RMS error of the example DQE estimate.

Conclusions

DQE and NEQ are not measured directly, but estimated from the results of several image measurements. The analysis presented allows the interpretation of measurement error statistics in terms of their combined effect on the DQE and NEQ estimates. The unique noise characteristics of each instrument and data processing method must be quantified. The expressions derived for the bias, variance, and RMS error are simple functions of the coefficients of variation associated with the measured MTF, γ, etc. In a calculated example, practical levels of measurement errors are shown to result in significant DQE estimation errors. Efforts to improve DQE and NEQ estimates, either by smoothing, instrumentation modifications, or measurement data processing, can be quantified in terms of the resulting bias, variance, and RMS error.

References

1. Jones, R. C., "Quantum Efficiency of Photographic Negatives," Adv. Electron. Electron Phys., 11: 87-183 (1959).
2. Fellgett, P. B., "On the Necessary Measurements for the Characterization and Optimum Use of Photographic Materials for Scientific Purposes," J. Photogr. Sc., 9: 201-206 (1961).
3. Shaw, R., "The Equivalent Quantum Efficiency of the Photographic Process," J. Photogr. Sc., 11: 199-204 (1963).
4. Rose, A., Vision: Human and Electronic, Plenum, New York, 1974.
5. Sandrick, J. M. and Wagner, R. F., "Absolute Measures of Physical Image Quality: Measurement and Application to Radiographic Magnification," Med. Phys., 9: 540-549 (1982).
6. Bunch, P. C., "Comparison of Signal-to-Noise Ratios for Some New Screen-Film Systems," Proc. SPIE, 486: 99-107 (1984).
7. Wagner, R. F., "Low Contrast Sensitivity of Radiographic, CT, Nuclear Medicine, and Ultrasound Medical Imaging Systems," IEEE Trans. Med. Imag., MI-2: 105-121 (1983).

8. Wagner, R. F. and Muntz, E. P., "Detective Quantum Efficiency (DQE) Analysis of Electrostatic Imaging and Screen-Film Imaging Mammography," Proc. SPIE, 173: 162-165 (1979).
9. Shaw, R., "Fundamental Image Quality Parameters for Xeroradiography," in The Physics of Medical Imaging: Recording System Measurement and Techniques, A. G. Haus, Ed., A.I.P., New York, 1979, pp. 231-238.
10. Shaw, R. and VanMetter, R. L., "An Analysis of the Fundamental Limitations of Screen-Film Systems for X-ray Detection. I. General Theory II. Model Calculations," Proc. SPIE, 454: 128-141 (1984).
11. Fu,T.-Y. and Roehrig, H., "Noise Power Spectrum, MTF, and DQE of Photoelectronic Radiographic Systems," Proc. SPIE, 454: 377-386 (1984).
12. Nishikawa, R. M. and Yaffe, M. J., "Signal-to-Noise Properties of Mammographic Film-Screen Systems," Med. Phys., 12: 32-39 (1985).
13. Fisher, M. G., "MTF, Noise-Power and DQE of Radiographic Screens," Photogr. Sci. Eng., 26: 33-41 (1982).
14. Dainty, J. C. and Shaw, R., Image Science, Academic Press, London, 1974, ch. 5.
15. Bunch, P. C., Huff, K. E., Shaw, R. and VanMetter, R. L., "Comparison of Theory and Experiment for the DQE of a Radiographic Screen-Film System," Proc. SPIE, 535: 166-183 (1985).
16. Bunch, P. C. and VanMetter, R. L., "Noise Characterization and Reduction in a Scanning Microdensitometer," in these Proceedings.
17. Lee, Y. and Dillon, P. L. P., "Cross Power Spectral Method for Improved Measurement of Film Noise," in these Proceedings.
18. Haus, A. G., Rossman, K., Vyborny, C., Hoffer, P. B., and Doi, K. "Sensitometry in Diagnostic Radiology, Radiometry and Nuclear Medicine," J. Appl. Photogr., 3: 114-124 (1977).
19. Haus, A. G., "Sensitometric Techniques in Medical Imaging," Proc. SPIE., 454: 83-104 (1984).
20. Bednarak, D. R., and Rudin, S., "Comparison of Modified Bootstrap and Conventional Sensitometry in Medical Radiography," Proc. SPIE, 233: 2-6 (1980).
21. Wagner, L. K., Haus, A. G., Barnes, G. T., Bencomo, J. A., and Amtey, S. R., "Comparison of Methods Used to Measure the Characteristic Curve of Radiographic Screen/Film Systems," Proc. SPIE, 233: 7-10 (1980).
22. Bencomo, J. A., and Haus, A. G., "Comparison of Intensity and Time Scale Sensitometric Methods for Evaluating Screen-Film Systems," Proc. SPIE, 173: 21-27 (1979).
23. Bunch, P. C. and Huff, K. E., "Signal-to-Noise Measurement on Two High-Resolution Screen-Film Systems," Proc. SPIE, 555: 68-83 (1985).
24. Doi, K., Holje, G., Loo, L.-N., Chan, H.-P., Sandrick, J. M., Jennings, R. J. and Wagner, R. F., "MTFs and Wiener Spectra of Radiographic Screen-Film Systems," U.S. Dept. Health Human Services Publ., FDA 82-8187, 1982.
25. Lubberts, G., "Some Aspects of the Square Wave Response Function of Radiographic Screen-Film Systems," Am. J. Roentgenol. Radium Ther. Nucl. Med., 106: 651-654 (1969).
26. Weiss, J. P., "Notes on Determining Modulation Transfer Data for X-ray Film-Screen Combinations," J. Appl. Photogr. Eng., 4: 82-84 (1978).
27. Dahle, M. E. and Haus, A. G., "Factors Affecting the Experimental Measurement and Modulation Calculation Including Deviation in Characteristic Curve Shape," Proc. SPIE., 233: 16-22 (1980).
28. Doi, K., Strubler, K. and Rossman, K, "Truncation Errors in Calculating the MTF of Radiographic Screen-Film Systems Using Line Spread Function," Phys. Med. Biol., 17: 241-250 (1972).
29. Sanderson, G. K., "Imaging Assessment: LSF and MTF," in The Physics of Medical Imaging: Recording System Measurement and Techniques, A. G. Haus, Ed., A.I.P., New York, 1979, pp. 118-137.
30. Bunch, P. C. and Sanderson, G. K., "Experimental Considerations and Data Analysis Techniques for Radiographic MTF Measurements," Image Analysis Techniques and Application, SPSE conference Tucson, Arizona, 1981, pp. 118-120.
31. Uchida, S., Inatsu, H, Kojima, K. and Tanaka, K., "Line Spread Functions by the Pre-exposure and Multiple-exposure Methods," Phys. Med. Biol., 31: 1275-1279 (1986).
32. Villafana, T., "Effect of Microdensitometer Scan Slit Misallignment in MTF Determination," Med. Phys., 2: 255-258 (1975).
33. Metz, C. E., Strubler, K. A. and Rossman, K., "Choice of Line Spread Function Sampling Distance for Computing the MTF of Radiographic Screen-Film Systems," Phys. Med. Biol., 17: 638-647 (1972).

34. Burgess, A. E., "An Empirical Equation for Screen MTFs," Med. Phys., 5: 199-204 (1978).
35. Bencomo, J. A., LeDuc, T., McGraw, F. J., Fallone, B. G. and Willis, C. E., "Logit Analysis of Screen-Film Modulation Transfer Data," J. Imag. Sci., 30: 270-273 (1986).
36. Sandrick, J. M. and Wagner, R. F., "Radiographic Screen-Film Noise Power Spectrum: Variation with Microdensitometer Slit Length," Appl. Opt., 20: 2795-2798 (1981).
37. Dainty and Shaw, op. cit., chapt. 8.
38. Wagner, R. F., "Fast Fourier Digital Quantum Mottle Analysis with Application to Rare Earth Intensifying Screen Systems," Med. Phys., 4: 157-162 (1977).
39. Vranckx, J., Breesch, P. and DeBelder, M., "Two-Dimensional Noise Power Spectra of Screen-Film Systems," Photogr. Sci. Eng., 28: 134-135 (1984).
40. Trabka, E. A. and Bunch, P. C., "Application of Maximum Entropy Spectrum Analysis to the Measurement of Low Frequency Radiographic Noise," Proc. SPIE., 454: 142-153 (1984).
41. Shaw, R. and Rabbani, M., "A Comparison of Physical Autocorrelation and Digital Wiener Spectrum Techniques for Screen-Film Evaluation," Proc. SPIE., 626: 76-81 (1986).
42. Bunch, P. C., Huff, K. E. and VanMetter, R. L., "Sources of Noise in High-Resolution Screen-Film Radiography," Proc. SPIE., 626: 64-75 (1986).
43. Burns, P. D. and Levine, B. L., "Wiener Spectrum Estimation at Zero Frequency via Direct Digital Computation," J. Appl. Photogr. Eng., 9: 78-82 (1983).
44. Sandrick, J. M., Wagner, R. F. and Hansen, K. M., "Radiographic Screen-Film Noise Power Spectrum: Calibration and Intercomparison," Appl. Opt., 21: 3597-3601 (1982).
45. Bunch, P. C., Shaw, R. and VanMetter, R. L., "Signal-to-Noise Measurement for a Screen-Film System," Proc. SPIE., 454: 154-163 (1984).
46. For example, Papoulis, A., Probability, Random Variables, and Stochastic Processes, McGraw-Hill, New York, 1965, pp. 151-152, 211-212.

Appendices

I. Moments of a function of zero-mean random variables

We are given a function of two independent random variables, $f(x,y)$, where the corresponding means and variances are μ_x, μ_x, σ_x^2, and σ_y^2. The mean values can be interpreted as the true values so, for example, $\hat{x}_i$ is the ith unbiased noisy measurement of μ_x. In the following expressions for the mean and variance of f, we retain only up to the second-order moments of x and y. The results can be generalized and applied to functions of more than two independent random variables. The ith observation of x is

$$\hat{x}_i = \mu_x + \Delta x_i, \tag{19}$$

where Δx is a zero-mean, wide-sense stationary random variable and μ_x is the true value. We expand f in a Taylor series about μ_x and μ_y,

$$\begin{aligned} f(\hat{x},\hat{y}) &= f(\mu_x,\mu_y) + f'_x(\hat{x}-\mu_x) + f'_y(\hat{y}-\mu_y) \\ &\quad + \frac{1}{2}\left\{f''_{xx}(\hat{x}-\mu_x)^2 + 2f''_{xy}(\hat{x}-\mu_x)(\hat{y}-\mu_y) + f''_{yy}(\hat{y}-\mu_y)^2\right\}\ldots \end{aligned}$$

where

$$f'_x = \left.\frac{\partial f(x,y)}{\partial x}\right|_{\mu_x,\mu_y}$$

and

$$f''_{xy} = \left.\frac{\partial^2 f(x,y)}{\partial x \partial y}\right|_{\mu_x,\mu_y}$$

Taking expectations and noting that x and y are independent,

$$E[f(\hat{x},\hat{y})] = f(\mu_x,\mu_y) + \frac{1}{2}\left\{f''_{xx}\sigma_x^2 + f''_{yy}\sigma_y^2\right\}. \tag{20}$$

The second term is the bias, $b1_f$.

The variance of f can be expressed as

$$\sigma_f{}^2 = E[f^2] - E[f]^2. \tag{21}$$

First we express f^2 in terms of the series,

$$\begin{aligned} f^2(\hat{x},\hat{y}) &= f^2(\mu_x,\mu_y) + (f'_x(\hat{x}-\mu_x))^2 + (f'_y(\hat{y}-\mu_y))^2 \\ &\quad + 2\,f(\mu_x,\mu_y)\left\{ f'_x(\hat{x}-\mu_x) + f'_y(\hat{y}-\mu_y) + \frac{f''_{xx}(\hat{x}-\mu_x)^2}{2} \right. \\ &\quad \left. + f''_{xy}(\hat{x}-\mu_x)(\hat{y}-\mu_y) + \frac{f''_{yy}(\hat{y}-\mu_y)^2}{2} \right\}. \end{aligned}$$

Taking expectations,

$$E[f^2(\hat{x},\hat{y})] = f^2(\mu_x,\mu_y) + f'_x{}^2\sigma_x{}^2 + f'_y{}^2\sigma_y{}^2 + f(\mu_x,\mu_y)\,[f''_{xx}\sigma_x{}^2 + f''_{yy}\sigma_y{}^2]. \tag{22}$$

Substituting equations (20) and (22) into (21),

$$\sigma_f{}^2 = f'_x{}^2\sigma_x{}^2 + f'_y{}^2\sigma_y{}^2. \tag{23}$$

II. Bias of a function of biased random variables

We are given the function, $f(x,y)$, of two random variables (measurements) that are corrupted with a bias error. The expected value of x is

$$E[\hat{x}] = b_x + \mu_x.$$

We define the bias of $f(x,y)$ as in equation (5):

$$b_f = E[f(\hat{x},\hat{y})] - f(\mu_x,\mu_y). \tag{24}$$

As in Appendix I, we can can expand f about the point (μ_x,μ_y). Taking expectations,

$$\begin{aligned} E[f(\hat{x},\hat{y})] &= f(\mu_x,\mu_y) + f'_x b_x + f'_y b_y \\ &\quad + \frac{1}{2}\left\{ f''_{xx}(\sigma_x{}^2 + b_x{}^2) + 2f''_{xy}b_x b_y + f''_{yy}(\sigma_y{}^2 + b_y{}^2) \right\}. \end{aligned} \tag{25}$$

The bias, found by substituting equation (25) into (24), is the sum of two components: one due to the variation of the measurements, $b1_f$, and the other due to their bias, $b2_f$. These are given by

$$b_f = b1_f + b2_f,$$

where

$$b1_f = \frac{1}{2}\left\{ f''_{xx}\sigma_x{}^2 + f''_{yy}\sigma_y{}^2 \right\} \tag{26}$$

$$b2_f = f'_x b_x + f'_y b_y + \frac{f''_{xx}b_x{}^2}{2} + f''_{xy}b_x b_y + \frac{f''_{yy}b_y{}^2}{2}. \tag{27}$$